Molecular Pharmacology Fast Forward. Published on July 24, 2012 as doi: 10.1124/mol.112.079376
This article has not been copyedited and formatted. The final version may differ from this version.

Sustained activation of NMDA receptors in podoctyes leads to oxidative stress, mobilization of TRPC6 channels, NFAT activation, and apoptotic cell death

Eun Young Kim, Marc Anderson, and Stuart E. Dryer

Department of Biology and Biochemistry, University of Houston, Houston, TX (EYK, MA, SED)

Department of Medicine, Division of Nephrology, Baylor College of Medicine, Houston, TX (SED)

Molecular Pharmacology Fast Forward. Published on July 24, 2012 as DOI: 10.1124/mol.112.079376
This article has not been copyedited and formatted. The final version may differ from this version.

Running title: NMDA signals through TRPC6 channels in podocytes

Address Correspondence to: Dr. Stuart E. Dryer, Department of Biology and Biochemistry, University of Houston, 4800 Calhoun, Houston, TX, 77204-5001, Tel 713-743-2697, FAX 713-473-2632, Email, SDryer@uh.edu

Text pages	38
Figures	9
References	60
Words in Abstract	249
Words in Introduction	737
Words in Discussion	1499

Non-standard abbreviations

CsA	Cyclosporine
DAPI	4'-6-Diamidino-2-phenylindole
FSGS	Focal and segmental glomerulosclerosis
L-HCA	L-homocysteic acid
MK-801	Dizocilpine
MnTBAP	Manganese (III) tetrakis (4-benzoic acid) porphyrin chloride
NFAT	Nuclear factor of activated T-cells
NMDA	*N*-methyl-*D*-aspartic acid
NOX	NADPH oxidase
OAG	1-oleoyl-2-acetyl-*sn*-glycerol
ROS	Reactive oxygen species
SKF-96365	1-[2-(4-Methoxyphenyl)-2-[3-(4-methoxyphenyl)propoxy]ethyl]imidazole 1-[β-(3-(4-Methoxyphenyl)propoxy)-4-methoxyphenethyl]-1*H*-imidazole hydrochloride
TUNEL	Terminal deoxynucleotidyl transferase dUTP nick-end labeling
TRPC5	Transient receptor potential canonical-5
TRPC6	Transient receptor potential canonical-6

Molecular Pharmacology Fast Forward. Published on July 24, 2012 as DOI: 10.1124/mol.112.079376
This article has not been copyedited and formatted. The final version may differ from this version.

Abstract

Atypical NMDA receptors are expressed in podocytes. Sustained (≥ 24 hr) application of 50-100 μM NMDA to immortalized mouse podocytes evoked a marked increase in the production of reactive oxygen species (ROS) such as H_2O_2. This effect of NMDA was associated with increased cell-surface expression of $p47^{(phox)}$, a cytosolic regulatory subunit of the NADPH oxidase NOX2. NMDA-evoked generation of ROS drove an increase in steady-state surface expression of TRPC6 channels, which was blocked by the NMDA antagonist MK-801 and by a membrane-permeable scavenger of ROS. The effect of NMDA on TRPC6 was observed using cell-surface biotinylation assays, and also with whole-cell recordings made under conditions designed to facilitate detection of current through TRPC6. NMDA mobilization of TRPC6 channels was blocked by concurrent treatment with the NMDA antagonist MK-801, and by a membrane-permeable scavenger of ROS. Mobilization of TRPC6 was also evoked by L-homocysteic acid (L-HCA). NMDA treatment also increased nuclear localization of endogenous NFAT, which could be blocked by MK-801, by scavenging ROS, by the calcineurin inhibitor cyclosporine, and by the TRPC channel inhibitor SKF-96365. NMDA treatment also evoked robust activation of Rho but not Rac, consistent with previous studies of downstream effectors of TRPC6 activation. Exposing cells to NMDA for 24 hr reduced total and cell surface expression of podocyte markers nephrin and podocin but there was no loss of cells. With longer NMDA exposure (72 hr) we observed loss of cells associated with nuclear fragmentation and increased expression of caspase-3, caspase-6 and Bax, suggesting an apoptotic process.

Molecular Pharmacology Fast Forward. Published on July 24, 2012 as DOI: 10.1124/mol.112.079376
This article has not been copyedited and formatted. The final version may differ from this version.

Introduction

Podocytes comprise one of several essential components of the glomerular filtration barrier (Pavenstädt et al., 2003). Primary processes extending from the podocyte cell body ramify and wrap around the glomerular capillary. A series of small foot processes extend from the major processes of podocytes and attach to the external face of the basement membrane of the glomerular capillary. Specialized junctions between adjacent foot processes, known as slit diaphragms, provide a permselective pathway that allows convective movement and diffusion of water and small solutes into the urinary space, while excluding macromolecules.

Structural alterations in podocyte foot processes occur in many glomerular diseases, leading to loss or displacement of slit diaphragms (Shirato, 2002). Sustained elevation of Ca^{2+} influx into podocytes may represent a common pathway driving these changes (Lavin and Winn, 2011). A landmark observation was the discovery that gain-of-function mutations in TRPC6 channels can cause familial forms of focal and segmental glomerulosclerosis (FSGS) (Winn et al., 2005; Reiser et al., 2005). A similar pathology is observed in mice over-expressing wild-type or mutant TRPC6 channels selectively in podocytes (Krall et al., 2009).

TRPC6 channels are not the only possible pathway for Ca^{2+} influx into podocytes. In addition to other members of the TRPC family (Tian et al., 2010), ionotropic NMDA receptors provide a potential pathway for Ca^{2+} influx into these cells (Rastaldi et al., 2006; Anderson et al., 2011). NMDA receptors were originally identified in neurons, where they are normally activated by synaptic release of glutamate.

Molecular Pharmacology Fast Forward. Published on July 24, 2012 as DOI: 10.1124/mol.112.079376
This article has not been copyedited and formatted. The final version may differ from this version.

Activated NMDA receptors show varying degrees of permeability to Ca^{2+} (Jahr and Stevens, 1993), which plays an important role in driving the downstream consequences of NMDA receptor activation.

NMDA receptors have been intensively studied in neuronal cells for two reasons: First, their activation induces several forms of synaptic plasticity in adult (Bliss and Collingridge, 1993) and developing (Cline and Constantine-Paton, 1989) nervous systems. Second, excessive NMDA receptor activation initiates a process known as excitotoxicity, resulting in death of neurons and glia driven in part by Ca^{2+} overload (Choi, 1992; Hardingham, 2009). Excitotoxicity is also associated with increased production of reactive oxygen species (ROS) (Kishida et al., 2005; Girouard et al., 2009). Excitotoxiticy can be produced by several endogenously occurring amino acids that activate NMDA receptors, including dicarboxylic acids, sulfur-containing amino acids derived from methionine metabolism, and by products of the kynurenine pathways of tryptophan metabolism (Olney et al., 1987; Kim et al., 1987).

It is now known that NMDA receptors are expressed in many different peripheral tissues (Patton et al., 1998, Parisi et al., 2009, Mashkina et al., 2010, Makhro et al., 2010; Tyagi et al., 2010), including podocytes (Rastaldi et al., 2006; Anderson et al., 2011), although their normal physiological functions in these tissues are not well understood. We have recently characterized the functional properties of NMDA receptors of podocytes (Anderson et al., 2011). These receptors are strongly activated by NMDA, and are blocked by D-aminophosphonovaleric acid and MK-801. Responses to NMDA are potentiated by D-serine and are nearly eliminated by an inhibitor of glycine and D-serine binding sites on NR1 subunits. As with neuronal NMDA receptors, the

Molecular Pharmacology Fast Forward. Published on July 24, 2012 as DOI: 10.1124/mol.112.079376
This article has not been copyedited and formatted. The final version may differ from this version.

podocyte receptors are permeable to Ca^{2+} and subjected to voltage-dependent inhibition by Mg^{2+}. However, podocyte NMDA receptors also exhibit several unusual features. The most significant is the fact that they cannot be activated by L-glutamate or L-aspartate (Anderson et al., 2011). Thus, although there is evidence that L-glutamate can be locally secreted by podocytes (Giardino et al., 2009), it seems likely that it acts primarily on metabotropic glutamate receptors (Puliti et al., 2011; Gu et al., 2012). However podocyte NMDA receptors are robustly activated by L-homocysteic acid (L-HCA), an endogenously occurring product of methionine metabolism (Anderson et al., 2011). These metabolites are elevated in hypertension, diabetes, and chronic kidney diseases (Jager et al., 2001; Francis et al., 2004) and can reach levels sufficient to activate NMDA receptors in vivo (Tyagi et al., 2010), especially in chronic kidney disease (Heinz et al., 2010).

In the present study we have characterized pathways whereby activation of podocyte NMDA receptors could lead to glomerular dysfunction. We have observed that podocyte NMDA receptors leads to increased NOX-dependent production of reactive oxygen species (ROS), which stimulate increased surface expression of functional TRPC6 channels. This in turn evokes a cyclosporine (CsA)-sensitive movement of nuclear factor of activated T-cells (NFAT) into the nucleus. NMDA receptor activation also caused a fall in the expression of nephrin and podocin, and, after 72 hours, can evoke apoptotic cell death.

Molecular Pharmacology Fast Forward. Published on July 24, 2012 as DOI: 10.1124/mol.112.079376
This article has not been copyedited and formatted. The final version may differ from this version.

Materials and Methods

Cell culture protocols, transfection, and drugs.

Cell culture protocols have been described previously (Kim et al., 2008, 2009, 2010, 2012). Briefly, the MPC-5 mouse podocyte cell line (obtained from Dr. Peter Mundel) was propagated at 33°C in RPMI-1640 medium supplemented with 10% fetal bovine serum and 100 U/ml penicillin-streptomycin, with recombinant mouse γ-interferon (Sigma), in humidified 5% CO_2 incubators. Podocyte differentiation and expression of podocyte markers was induced by removal of γ-interferon and temperature switch to 37°C for 14 days. NMDA, L-HCA, MK-801, SKF96365 and CsA were obtained from Sigma. Manganese (III) tetrakis (4-benzoic acid) porphyrin chloride (MnTBAP) was obtained from Oxis International.

Assay of ROS generation.

Generation of H_2O_2 by podocytes was measured using the OxiSelect™ fluorometric assay (Cell Biolabs Inc.) according to the manufacturer's instructions, as described previously in detail (Kim et al., 2012). In this assay H_2O_2 in the presence of horseradish peroxidase causes oxidation of 10-acetyl-3,7-dihydroxyphenoxazine to resorufin, a fluorescent product with a high extinction coefficient, which could be measured using a fluorescence microplate reader.

Immunoblot analysis, cell-surface biotinylation assays, and nuclear localization of NFAT.

Immunoblot analysis and cell-surface biotinylation were carried out using standard methods as described in detail previously (Kim et al., 2008, 2009, 2010, 2012). The

Molecular Pharmacology Fast Forward. Published on July 24, 2012 as DOI: 10.1124/mol.112.079376
This article has not been copyedited and formatted. The final version may differ from this version.

primary antibodies were rabbit anti-TRPC6 (Alomone), Rabbit anti-p47$^{(phox)}$ and rabbit anti-NOX2 (Santa Cruz), rabbit anti-NOX4 (Epitomics), rabbit anti-podocin (Santa Cruz), rabbit anti-nephrin (Abcam) and mouse monoclonal anti-β-actin (Millipore). For cell-surface biotinylation assays, intact podocytes were treated with a membrane impermeable biotinylation reagent, sulfo-*N*-hydroxy-succinimidobiotin (Pierce Biotechnology, Rockford, IL) (1 mg/ml) for 1 h. The reaction was stopped, cells were lysed, and biotinylated proteins from the cell surface were recovered by incubation with immobilized streptavidin-agarose beads. A sample of the initial cell lysate was retained for analysis of total proteins, and in some experiments of β-actin. These samples were quantified by immunoblot analysis followed by densitometric analysis using Image J™ software. Bar graphs describing these data were constructed from 3-5 repetitions of each experiment. NFAT localization in podocyte nuclei was measured using a commercial assay (Active Motif) and a nuclear extract kit purchased from the same manufacturer. In this assay we also used a mouse monoclonal anti-histone and a mouse monoclonal anti-β-actin (Millipore). In separate experiments on NFAT localization, podocytes were subjected to various treatments and fixed in 4% paraformaldehyde at room temperature for 10 minutes. Fixed cells were permeablized, blocked and incubated with rabbit anti-NFATc1 (Active Motif) and nuclei were counterstained with 4'-6-diamidino-2-phenylindole (DAPI) for 1 hour at 37°. After washing, cells were treated with AlexaFlour 488-conjugated anti-rabbit IgG (Molecular Probes), and then rinsed, mounted, and images were collected on an Olympus FV-1000 inverted stage confocal microsope using a Plan Apo N 60X 1.42NA oil-immersion objective, and processed by FluoView™ software.

Molecular Pharmacology Fast Forward. Published on July 24, 2012 as DOI: 10.1124/mol.112.079376
This article has not been copyedited and formatted. The final version may differ from this version.

Electrophysiology. Whole-cell recordings were made as described previously (Kim et al., 2012) from control cells and from cells that had been exposed for 24 hr to NMDA, or a combination of NMDA and inhibitors. All cells were treated with 100 μM 1-oleoyl-2-acetyl-*sn*-glycerol (OAG) for 15 min prior to whole-cell recordings. This diacylglycerol analog does not activate TRPC5 (Hofmann et al., 1999) and we have previously shown that responses to OAG in podocytes are abolished after TRPC6 knockdown (Kim et al., 2012). In all recordings, the bath solution contained 150 mM NaCl, 5.4 mM CsCl, 0.8 mM $MgCl_2$, 5.4 mM $CaCl_2$, and 10 mM HEPES, pH 7.4. Pipette solutions contained 10 mM NaCl, 125 mM CsCl, 6.2 mM $MgCl_2$, 10 mM HEPES, and 10 mM EGTA, pH 7.2. Currents were evoked by a ramp voltage commands (-80 to + 80 mV over 2.5 sec) from a holding potential of -40 mV. In each cell, currents were measured before and after superfusion of 50 μM La^{3+}, which blocks TRPC6 channels but not TRPC5, in poodcytes (Tian et al., 2010) or before and after 50 μM SKF-96365. Data were digitized using a Digidata™ interface (Molecular Devices), and stored for off-line analysis using PClamp™ software (Molecular Devices). La^{3+}-sensitive currents were obtained by digital subtraction, and the peak measured at +80 mV was used for quantitative analysis of the effects of previous NMDA and drug treatments.

Analysis of podocyte cell death and small GTPases. Rho and Rac activation were measured using commercial glutathione-*S*-transferase pull-down assays from Cytoskeleton Inc. according to the manufacturer's instructions. Analyses of apoptosis markers were carried out using rabbit antibodies against caspase-3, caspase 6, Bax, and Bcl-XL (Cell Signaling). Nuclear fragmentation was detected using a commercial immunofluorescence-based apoBrdU™ terminal deoxynucleotidyl transferase dUTP

Molecular Pharmacology Fast Forward. Published on July 24, 2012 as DOI: 10.1124/mol.112.079376
This article has not been copyedited and formatted. The final version may differ from this version.

nick-end labeling (TUNEL) assay (Invitrogen). In addition, overall cell viability was determined using the Cytoselect™ assay (Cell Biolabs Inc.) and by measuring release of lactate dehydrogenase into media using an assay from Roche Applied Science.

Molecular Pharmacology Fast Forward. Published on July 24, 2012 as DOI: 10.1124/mol.112.079376
This article has not been copyedited and formatted. The final version may differ from this version.

Results

All of these experiments were carried out on the differentiated cells of an immortalized mouse podocyte cell line, which express functional NMDA receptors (Anderson et al., 2011) along with many other podocyte markers (Kim et al., 2008, 2009, 2010). Initial experiments were motivated by previous reports that activation of neuronal NMDA receptors leads to increased production of reactive oxygen species (ROS) (Kishida et al., 2005; Girouard et al., 2009). We observed that exposure to NMDA increased production of ROS in podocytes using a fluorometric assay based on production of a highly fluorescent product in the presence of horseradish peroxisase (Fig. 1A). This assay primarily detects production of H_2O_2, and we observed that 24 hr of exposure to 100 μM NMDA caused a marked increase in H_2O_2 production that was maintained with longer exposures up to 72 hr. However, a 6-hr exposure to NMDA did not produce a detectable increase in bulk cytosolic H_2O_2 above that seen in untreated cells. The NMDA-evoked increase in H_2O_2 was not seen in cells concurrently treated with 100 μM manganese (III) tetrakis (4-benzoic acid) porphyrin chloride (MnTBAP), a membrane-permeable mimetic of superoxide dismutase (Batinić-Haberle, 2002) and catalase (Day et al., 1997) that we have used previously in studies of mouse podocytes (Kim et al., 2012).

ROS are produced as a product of various NADPH oxidases, which have been implicated in NMDA receptor-mediated excitotoxic responses in neurons (Kishida et al., 2005; Girouard et al., 2009). The NADPH oxidase NOX2 is normally regulated by formation of complexes at the cell surface with cytosolic regulatory subunits, including

Molecular Pharmacology Fast Forward. Published on July 24, 2012 as DOI: 10.1124/mol.112.079376
This article has not been copyedited and formatted. The final version may differ from this version.

one known as p47$^{(phox)}$ (Bedard and Krause, 2007). Using cell-surface biotinylation assays, we observed that 24 hr treatment with NMDA resulted in a marked increase in the steady-state surface expression of p47$^{(phox)}$ that was blocked by concurrent treatment with the NMDA antagonist dizocilpine (MK-801) (Fig. 1C, D). By contrast, NMDA had no consistent effect on the steady-state surface expression of NOX2 or NOX4 (data not shown). Collectively, these data indicate that, as in neurons, NMDA receptor activation in podocytes results in oxidative stress associated with increased production of ROS that is mediated at least in part by modulation of an NADPH oxidase isoform.

Previous studies have shown that TRPC6 channels are redox-sensitive proteins (Wang et al., 2009; Graham et al., 2010), and we have shown that exogenous application of H_2O_2 and other treatments that increase generation of ROS result in increased surface expression of podocyte TRPC6 channels (Kim et al., 2012). In the present study we have observed that a 24-hr treatment with 50 or 100 μM NMDA caused a robust increase in the steady-state surface expression of podocyte TRPC6 channels (Fig. 2A). Moreover, this effect was blocked by concurrent application of MK-801 (Fig. 2B) or MnTBAP (Fig. 2C).

We also observed an increase in functional macroscopic currents with pharmacological properties of TRPC6 (Fig. 3). In these experiments, podocytes were treated with NMDA receptor agonists and antagonists for 24 hr. Cells were then treated with 100 μM OAG for 15 min prior to whole-cell recordings. OAG is a membrane-permeable analog of diacylglycerol that can activate TRPC6, TRPC3, and TRPC7 channels (Hofmann et al., 1999). We have previously shown that the OAG-evoked

Molecular Pharmacology Fast Forward. Published on July 24, 2012 as DOI: 10.1124/mol.112.079376
This article has not been copyedited and formatted. The final version may differ from this version.

macroscopic currents in podocytes are eliminated by TRPC6 knockdown (Kim et al., 2012). Whole-cell currents were evoked by 2.5-s duration ramp voltage commands (-80 to +80 mV) before and after application of 50 μM La^{3+} (Fig. 3A), which blocks TRPC6 channels but not TRPC5 channels in podocytes (Tian et al., 2010). The La^{3+}-sensitive components of the currents were obtained by digital subtraction in each cell and then quantified (Fig. 3B). We observed that La^{3+}-sensitive currents (measured at +80 mV) in cells previously exposed to NMDA were nearly 3-fold larger than those observed in untreated cells, and the effects of NMDA were blocked by concurrent treatment with either 10 μM MK-801 or 100 μM MnTBAP (Fig. 3A, B). In addition, we observed that the currents recorded using these protocols were almost completely inhibited by 50 μM SKF-96365 (Fig. 3C), an agent that blocks cationic channels in the TRPC family, and which nearly eliminates TRPC6 currents in podocytes at this concentration (Kim et al., 2012). It is important to note that in these experiments, NMDA treatments were completed prior to electrophysiology and NMDA was not present at the time the recordings were made. Collectively, these results indicate that NMDA-evoked generation of ROS results in mobilization of functional TRPC6 channels. The electrophysiological data are therefore consistent with the results of cell surface biotinylation assays.

These observations raised the possibility that sustained activation of NMDA receptors in podocytes can engage functionally significant pathways that are downstream of TRPC6. One such pathway entails activation of nuclear factor of activated T-cells (NFAT) (Schlöndorff et al., 2009). Highly phosphorylated NFAT normally resides in the cytosol. However, TRPC6-mediated activation of calcineurin

Molecular Pharmacology Fast Forward. Published on July 24, 2012 as DOI: 10.1124/mol.112.079376
This article has not been copyedited and formatted. The final version may differ from this version.

results in dephosphorylation of NFAT, causing some of it to translocate to the nucleus where it can regulate gene expression (Scott et al., 1997; Kuwahara et al., 2006). Using an assay based on cell fractionation, we observed that 100 μM NMDA treatment for 24 hr caused a marked increase in the amount of NFAT that is located in nuclei (a cell fraction enriched in histone), but did not produce a substantial effect on cytosolic NFAT (a much larger pool in a cell fraction in which actin is abundant) (Fig. 4A). This effect of NMDA was blocked by concurrent exposure to 10 μM MK-801. It was also blocked by 50 μM SKF-96365. It bears noting that SKF-96365 does not block NMDA receptors in neurons (Zhu et al., 2005), and this result suggests that mobilization of TRPC6 underlies this response to NMDA. Stimulatory effects of NMDA could also be seen using confocal microscopy to examine localization of NFAT after drug treatments (Fig. 4B). These experiments showed that NMDA treatment increased the nuclear localization of NFAT, and that this effect was blocked by concurrent treatment with MK-801 and SKF-96365. Using the same methods, we also observed that the effects of NMDA on nuclear localization of NFAT were also blocked by concurrent treatment with 10 μM CsA, an inhibitor of the phosphatase calcineurin (Fig. 5).

One significant consequence of activation of TRPC6-calcineurin signaling cascades in podocytes is modulation of small GTPases (Greka and Mundel, 2012). We have previously shown that NMDA can cause activation of Rho, which we have repeated in the present studies (Fig. 6A). We have extended these observations to show that NMDA treatment for 24 hr produces much less Rac activation (Fig. 6B). Rac activation in podocytes is reported to be preferentially coupled to TRPC5 signaling cascades (Tian et al., 2010). Another consequence of NMDA treatment for 24 hr is an

Molecular Pharmacology Fast Forward. Published on July 24, 2012 as DOI: 10.1124/mol.112.079376
This article has not been copyedited and formatted. The final version may differ from this version.

apparent de-differentiation or loss of cell function as evidenced by a marked fall in total expression of the podocyte markers nephrin and podocin relative to actin, and an even larger relative decrease in the steady-state surface expression of these membrane proteins (Fig. 7). This cannot be explained by a loss of viable cells, at least at 24 hr. Thus, we observed that normal numbers of cells are still present after 24 hr of NMDA treatment (Fig. 8A), which indicates that these cells are remarkably resistant to excitotoxic effects of NMDA compared to neurons (Choi, 1992). However, 72 hr of continuous exposure to NMDA causes podocytes to die as evidenced by simply counting the number of cells that can be labeled with vital dyes (Fig. 8A) or by monitoring release of lactate dehydrogenase (LDH) into the medium (Fig. 8B). As in neurons (Hardingham, 2009), the cell death evoked by 72-hr NMDA treatment appears to be mediated in part by apoptosis. Thus, NMDA treatment resulted in marked fragmentation of podocyte DNA detected using immunofluorescence TUNEL assays (Fig. 8C). TUNEL signal was not detected in control cells or in cells treated with NMDA for 24 hr. In addition, NMDA treatment for 72 hr evoked increases in caspase 3, caspase 6, and Bax, and a fall in Bcl-XL, as measured by immunoblot (Fig. 8D).

NMDA is an artificial ligand—albeit one that is a highly selective agonist for NMDA receptors. The question arises as to whether an endogenously occurring NMDA receptor agonist can evoke similar effects. We observed that 24-hr exposure to 50 μM L-HCA evoked a robust increase in surface expression of TRPC6 channels as assessed by cell surface biotinylation assays, a response that was indistinguishable from that evoked by NMDA (Fig. 9A, B), as well as an increase in amplitudes of OAG-evoked TRPC6 currents (data not shown). We also observed that a 72-hr exposure to 50 μM L-

Molecular Pharmacology Fast Forward. Published on July 24, 2012 as DOI: 10.1124/mol.112.079376
This article has not been copyedited and formatted. The final version may differ from this version.

HCA evoked nuclear fragmentation similar to that evoked by NMDA (Fig. 9C), suggesting that this NMDA agonist can also evoke apoptotic cell death.

Molecular Pharmacology Fast Forward. Published on July 24, 2012 as DOI: 10.1124/mol.112.079376
This article has not been copyedited and formatted. The final version may differ from this version.

Discussion

In this study we have demonstrated a functional link between sustained activation of podocyte NMDA receptors and the mobilization of TRPC6 channels to the cell. Mobilization of TRPC6 channels appears to be driven by generation of ROS, and leads to engagement of associated downstream signaling cascades, including calcineurin, NFAT and Rho. Sustained activation of NMDA receptors also leads to reduced surface expression of the essential slit diaphragm proteins nephrin and podocin, and eventually induces apoptotic cell death. The pathways activated by NMDA may not be entirely in series. For example, it is likely that continuous production of ROS will exert deleterious effects on podocytes independent of TRPC6 mobilization, and calcineurin effects on Rho do not require activation of NFAT (Faul et al., 2008). However, coupling to TRPC6 is likely to amplify the adverse effects of sustained NMDA receptor activation.

In neurons, the NMDA-evoked generation of ROS is mediated by activation of the NADPH oxidase NOX2 (Kishida et al., 2005; Girouard et al., 2009). Our results suggest that a similar mechanism occurs in podocytes, as we observed increased surface expression of $p47^{(phox)}$ after 24 hr of NMDA treatment, and inhibition of NMDA effects by a ROS scavenger. By contrast we did not see marked increases in steady-state surface expression of NO2 or NOX4. Recall that $p47^{(phox)}$ is one of two cytosolic auxiliary subunits of NOX2, and its translocation to the cell surface is an essential step leading to activation of NOX2 catalytic activity (Bedard and Krause, 2007). Previous studies have shown that TRPC6 are redox-sensitive channels and that ROS affects both the gating and steady-state expression of these channels on the cell surface

Molecular Pharmacology Fast Forward. Published on July 24, 2012 as DOI: 10.1124/mol.112.079376
This article has not been copyedited and formatted. The final version may differ from this version.

(Wang et al., 2009; Graham et al., 2010; Kim et al., 2012). We have previously shown that generation of ROS via mobilization of the NADPH oxidase NOX4 contributes to insulin-evoked mobilization of TRPC6 channels, and we have proposed that this is a normal feature of insulin signaling in podocytes (Kim et al., 2012). Therefore, it is interesting that NMDA appears to mobilize podocyte TRPC6 channels through its actions on a different NADPH oxidase (NOX2). The mechanisms whereby NMDA receptor activation leads to activation of NOX2 are not clear. However, it is possible that there are multiple independently regulated populations of TRPC6 channels. In this regard, TRPC6 channels have been detected in the cell body and major processes of podocytes as well as at the slit diaphragm (Reiser et al., 2005; Huber et al., 2006), and TRPC6 channels are likely to reside in molecularly distinct complexes depending on their location in the cell (Roselli et al., 2002; Huber et al., 2006). It is also possible that transient elevations of ROS may play an important role in normal signaling cascades, but continuous elevation of these species may induce pathophysiological responses, as with Ca^{2+} signaling (Lavin and Winn, 2011).

The NMDA-evoked increase in surface expression of podocyte TRPC6 channels is associated with an increase in OAG-activated cationic currents in podocytes that are blocked by La^{3+} or SKF-96365. This effect of NMDA was abolished by concurrent exposure to the NMDA antagonist MK-801 and by quenching ROS. NMDA-evoked mobilization of TRPC6 channels also increased NFAT localization in podocyte nuclei. NFAT is a transcription factor that is regulated by the phosphatase calcineurin, which dephosphorylates NFAT and thereby allows its translocation to the nucleus (Scott et al., 1997). A contribution of TRPC6 channels to this pathway was initially established in

Molecular Pharmacology Fast Forward. Published on July 24, 2012 as DOI: 10.1124/mol.112.079376
This article has not been copyedited and formatted. The final version may differ from this version.

cardiac cells, where it is thought to play a role in angiotensin-mediated cardiac hypertrophy (Kuwahara et al., 2006). A role for NFAT in podocyte signaling was implicated by studies in cultured cells using a luminescent NFAT promoter (Schlöndorff et al., 2009; Nijenhuis et al., 2011), and it has been observed more recently that podocyte-specific over-expression of NFAT leads to albuminuria and glomerulosclerosis, along with reduced expression of nephrin and synaptopodin (Wang et al., 2010).

In the present study we observed that NMDA-evoked movement of endogenous NFAT to the nucleus was completely blocked by MK-801, and was also blocked by the TRPC inhibitor SKF-96365. We should note that SKF-96365 does not inhibit NMDA receptors (Zhu et al., 2005), and these data therefore suggest that the effects of NMDA on NFAT require amplification by TRPC channels. In this regard, we also observed partial inhibition of NMDA-evoked NFAT activation after TRPC6 knockdown using siRNA (data not shown), although we should also note that the TRPC6 knockdown in those experiments was not complete. We also blocked NMDA-evoked NFAT mobilization using CsA, confirming that calcineurin activation is an essential intermediate step in this cascade, as described previously (Schlöndorff et al., 2009; Wang et al., 2011). Calcineurin can also affect podocyte cytoskeleton in part through dephosphorylation of synaptopodin which in turn affects Rho signaling (Faul et al., 2008). A previous study has suggested that TRPC6 is preferentially coupled to RhoA signaling in podocytes, whereas TRPC5 is preferentially coupled to Rac1 (Tian et al., 2010). In the present study we confirmed that NMDA causes robust activation of Rho, consistent with the observed mobilization of TRPC6. In a separate set of experiments

Molecular Pharmacology Fast Forward. Published on July 24, 2012 as DOI: 10.1124/mol.112.079376
This article has not been copyedited and formatted. The final version may differ from this version.

we have observed that NMDA causes at least some mobilization of TRPC5 channels to the cell surface (data not shown), but for whatever reason this was not sufficient to cause activation of Rac. It is possible that Rac activation also requires activation or over-activation of angiotensin signaling systems in these cells (Tian et al., 2010). In any case, a role for TRPC5 in podocyte physiology has not as yet been established by in vivo experiments.

Treatment of podocytes with NMDA for 24 hr evoked a fall in total expression of both nephrin and podocin relative to actin. Notably, this treatment caused an even more striking decrease in the steady-state surface expression of these membrane proteins. A reduction in podocin and nephrin expression at the protein level is observed in several acquired glomerular diseases (Horinouchi et al., 2003; Koop et al., 2003), and may be a consequence NFAT activation (Wang et al., 2010). With even longer exposure to NMDA (72 hr), we observed apoptotic cell death based on several criteria. In this regard, sustained activation of calcineurin in podocytes can also lead to apoptosis (Wang et al., 2011). Similarly, ROS-mediated activation of TRPC6 has been implicated in podocyte pathology evoked by puromycin aminonucloside and this effect is sensitive to inhibition of NOX2 (Wang et al., 2009) suggesting that the combination of oxidative stress and Ca^{2+} overload is highly deleterious for the normal function of podocytes and their foot processes (Lavin and Winn, 2011). Nevertheless, it is notable that podocytes are much less sensitive to toxic effects of NMDA than neurons, which generally die within 6 hr of the onset of treatment.

Given all this, the question arises as to what physiological conditions might lead to sustained activation of podocyte NMDA receptors and the initiation of these

Molecular Pharmacology Fast Forward. Published on July 24, 2012 as DOI: 10.1124/mol.112.079376
This article has not been copyedited and formatted. The final version may differ from this version.

cascades? The NMDA receptors of podocytes are not activated by L-glutamate or L-aspartate, in very marked contrast to neuronal NMDA receptors (Anderson et al., 2011). The molecular basis for this anomalous feature is not understood, but it suggests that NMDA receptors are not part of the local glutamate signaling pathway recently identified in podocytes (Rastaldi et al., 2006; Giardino et al., 2009). That pathway instead appears to be mediated by metabotropic glutamate receptors (Puliti et al., 2011; Gu et al., 2012). Podocyte (Anderson et al., 2011) and neuronal (Olney et al., 1987; Kim et al., 1987) NMDA receptors are robustly activated by sulfur-containing derivatives of methionine metabolism, such as L-HCA. These metabolites are markedly elevated in chronic kidney disease (Massy, 2006; Potter et al., 2008), and can achieve circulating concentrations sufficient to activate NMDA receptors (Heinz et al., 2009, 2010). In this regard, deleterious effects of hyperhomocysteinemia on cardiac tissue are markedly reduced in mice with heart-specific knockdown of NMDA receptor NR1 subunits (Tyagi et al., 2010). In addition, a variety of treatments that lead to chronically elevated serum L-homocysteine levels in rodents result in glomerulosclerosis and effacement of podocyte foot processes (Yi et al., 2007; Zhang et al., 2010a, 2010b, 2011; Sen et al., 2010). Moreover, the glomeruosclerosis and proteinuria evoked by hyperhomocysteinemia can be reduced by in vivo administration of MK-801 (Zhang et al., 2010b) and suppressed by knockdown of auxiliary subunits of NOX-2 (Zhang et al., 2011). We have previously demonstrated that podocyte NMDA receptors are activated by L-HCA (Anderson et al., 2011), and in the present study we observed that L-HCA could also induce robust mobilization of TRPC6, as was seen with NMDA. As with NMDA, exposure to L-HCA for 72 hr also evoked nuclear fragmentation. These results

Molecular Pharmacology Fast Forward. Published on July 24, 2012 as DOI: 10.1124/mol.112.079376
This article has not been copyedited and formatted. The final version may differ from this version.

raise the possibility of a pathophysiological positive feedback loop in which elevated circulating L-homocysteine metabolites lead to NMDA receptor- and TRPC6-mediated glomerular damage and kidney disease. This could result in additional elevations in L-homocysteine and acceleration of nephropathy. It is possible that intervening in this vicious cycle through inhibition of either NMDA receptors or TRPC6 channels could slow the loss of nephrons, and may represent plausible strategies for treatment of chronic glomerulodegenerative diseases.

Molecular Pharmacology Fast Forward. Published on July 24, 2012 as DOI: 10.1124/mol.112.079376
This article has not been copyedited and formatted. The final version may differ from this version.

Authorship contributions

Participated in research design: Kim, Anderson, Dryer.

Conducted experiments: Kim, Anderson.

Performed data analysis: Kim, Anderson.

Wrote or contributed to the writing of the manuscript: Dryer, Kim.

Molecular Pharmacology Fast Forward. Published on July 24, 2012 as DOI: 10.1124/mol.112.079376
This article has not been copyedited and formatted. The final version may differ from this version.

References

Anderson M, Suh JM, Kim EY, and Dryer SE (2011) Functional NMDA receptors with atypical properties are expressed in podocytes. *Am J Physiol Cell Physiol* **300:**C22-32.

Batinić-Haberle I (2002) Manganese porphyrins and related compounds as mimics of superoxide dismutase. *Methods Enzymol* **349:**223-233.

Bedard K and Krause KH (2007) The NOX family of ROS-generating NADPH oxidases: physiology and pathophysiology. *Physiol Rev* **87:**245-313.

Bliss TV and Collingridge GL (1993) A synaptic model of memory: long-term potentiation in the hippocampus. *Nature* **361:**31-39.

Choi D (1992) Excitotoxic cell death *J Neurobiol* **23**:1261-76.

Cline HT and Constantine-Paton M (1989) NMDA receptor antagonists disrupt the retinotectal topographic map. *Neuron* **3:**413-326.

Day BJ, Fridovich I, and Crapo JD (1997) Manganic porphyrins possess catalase activity and protect endothelial cells against hydrogen peroxide-mediated injury. *Arch Biochem Biophys* **347:**256-262.

Faul C, Donnelly M, Merscher-Gomez S, Chang YH, Franz S, Delfgaauw J, Chang JM, Choi HY, Campbell KN, Kim K, Reiser J, and Mundel P (2008) The actin

cytoskeleton of kidney podocytes is a direct target of the antiproteinuric effect of cyclosporine A. *Nat Med* **14:**931-938.

Francis ME, Eggers PW, Hostetter TH, and Briggs JP (2004) Association between serum homocysteine and markers of impaired kidney function in adults in the United States. *Kidney Int* **66:**303-312.

Giardino L, Armelloni S, Corbelli A, Mattinzoli D, Zennaro C, Guerrot D, Tourrel F, Ikehata M, Li M, Berra S, Carraro M, Messa P, and Rastaldi MP (2009) Podocyte glutamatergic signaling contributes to the function of the glomerular filtration barrier. *J Am Soc Nephrol* **20:**1929-1940.

Girouard H, Wang G, Gallo EF, Anrather J, Zhou P, Pickel VM, and Iadecola C (2009) NMDA receptor activation increases free radical production through nitric oxide and NOX2. *J Neurosci* **29:**2545-2552.

Graham S, Ding M, Ding Y, Sours-Brothers S, Luchowski R, Gryczynski Z, Yorio T, Ma H, and Ma R (2010) Canonical transient receptor potential 6 (TRPC6), a redox-regulated cation channel*. J Biol Chem* **285:**23466-23476.

Greka A and Mundel P (2012) Cell biology and pathology of podocytes. *Annu Rev Physiol* **74:**299-323.

Gu Z, Liu W, Wei J, and Yan Z (2012) Regulation of *N*-Methyl-D-aspartic acid (NMDA) receptors by metabotropic glutamate receptor 7. *J Biol Chem* **287:**10265-10275.

Hardingham GE (2009) Coupling of the NMDA receptor to neuroprotective and neurodestructive events. *Biochem Soc Trans* **37:**1147-1160.

Heinz J, Kropf S, Luley C, and Dierkes J (2009) Homocysteine as a risk factor for cardiovascular disease in patients treated by dialysis: a meta-analysis. Am *J Kidney Dis* **54:**478-489.

Hofmann T, Obukhov AG, Schaefer M, Harteneck C, Gudermann T, Schultz G (1999) Direct activation of human TRPC6 and TRPC3 channels by diacylglycerol. Nature **397**:259-63.

Horinouchi I, Nakazato H, Kawano T, Iyama K, Furuse A, Arizono K, Machida J, Sakamoto T, Endo F, and Hattori S (2003) In situ evaluation of podocin in normal and glomerular diseases. *Kidney Int* **64:**2092-2099.

Huber TB, Kwoh C, Wu H, Asanuma K, Gödel M, Hartleben B, Blumer KJ, Miner JH, Mundel P, and Shaw AS (2006) Bigenic mouse models of focal segmental glomerulosclerosis involving pairwise interaction of CD2AP, Fyn, and synaptopodin. *J Clin Invest* **116:**1337-1345.

Jager A, Kostense PJ, Nijpels G, Dekker JM, Heine RJ, Bouter LM, Donker AJ, and Stehouwer CD (2001) Serum homocysteine levels are associated with the development of (micro)albuminuria: the Hoorn study. *Arterioscler Thromb Vasc Biol* **21:**74-81.

Jahr CE and Stevens CF (1993) Calcium permeability of the *N*-methyl-D-aspartate receptor channel in hippocampal neurons in culture. *Proc Natl Acad Sci U S A* **90:**11573-11577.

Kim EY, Choi KJ, and Dryer SE (2008) Nephrin binds to the COOH terminus of a large-conductance Ca^{2+}-activated K^+ channel isoform and regulates its expression on the cell surface*. Am J Physiol Renal Physiol* **295:**F235-246.

Kim EY, Chiu YH, and Dryer SE (2009) Neph1 regulates steady-state surface expression of Slo1 Ca^{2+}-activated K^+ channels: different effects in embryonic neurons and podocytes. *Am J Physiol Cell Physiol* **297:**C1397-1388.

Kim EY, Suh JM, Chiu YH, and Dryer SE (2010) Regulation of podocyte BK_{Ca} channels by synaptopodin, Rho, and actin microfilaments. *Am J Physiol Renal Physiol* **299:**F594-604.

Kim EY, Anderson M, and Dryer SE (2012) Insulin increases surface expression of TRPC6 channels in podocytes: role of NADPH oxidases and reactive oxygen species. *Am J Physiol Renal Physiol* **302:**F298-307.

Kim JP, Koh JY, and Choi DW (1987) L-homocysteate is a potent neurotoxin on cultured cortical neurons. *Brain Res* **437:**103-110.

Kishida KT, Pao M, Holland SM, and Klann E (2005) NADPH oxidase is required for NMDA receptor-dependent activation of ERK in hippocampal area CA1. *J Neurochem* **94:**299-306.

Koop K, Eikmans M, Baelde HJ, Kawachi H, De Heer E, Paul LC, and Bruijn JA (2003) Expression of podocyte-associated molecules in acquired human kidney diseases. *J Am Soc Nephrol* **14:**2063-2071.

Krall P, Canales CP, Kairath P, Carmona-Mora P, Molina J, Carpio JD, Ruiz P, Mezzano SA, Li J, Wei C, Reiser J, Young JI, and Walz K (2010) Podocyte-specific overexpression of wildtype or mutant TRPC6 in mice is sufficient cause glomerular disease. *PLoS One* **5:**e12859.

Kuwahara K, Wang Y, McAnally J, Richardson JA, Bassel-Duby R, Hill JA, and Olson EN (2006) TRPC6 fulfills a calcineurin signaling circuit during pathologic cardiac remodeling. *J Clin Invest* **116:**3114-3126.

Lavin PJ and Winn MP (2011) TORCing up the importance of calcium signaling. *J Am Soc Nephrol* **22:**1391-1393.

Makhro A, Wang J, Vogel J, Boldyrev AA, Gassmann M, Kaestner L, and Bogdanova A (2010) Functional NMDA receptors in rat erythrocytes. *Am J Physiol Cell Physiol* **298:**C1315-1325.

Mashkina AP, Cizkova D, Vanicky I, and Boldyrev AA (2010) NMDA receptors are expressed in lymphocytes activated both in vitro and in vivo. *Cell Mol Neurobiol* **30:**901-907.

Massy ZA (2006) Therapy of hyperhomocysteinemia in chronic kidney disease. *Semin Nephrol* **26:**24-27.

Merritt JE, Armstrong WP, Benham CD, Hallam TJ, Jacob R, Jaxa-Chamiec A, Leigh BK, McCarthy SA, Moores KE, and Rink TJ (1990) SK&F 96365, a novel inhibitor of receptor-mediated calcium entry. *Biochem J* **271:**515-522.

Nijenhuis T, Sloan AJ, Hoenderop JG, Flesche J, van Goor H, Kistler AD, Bakker M, Bindels RJ, de Boer RA, Möller CC, Hamming I, Navis G, Wetzels JF, Berden JH, Reiser J, Faul C, and van der Vlag J (2011) Angiotensin II contributes to podocyte injury by increasing TRPC6 expression via an NFAT-mediated positive feedback signaling pathway. *Am J Pathol* **179:**1719-1732.

Olney JW, Price MT, Salles KS, Labruyere J, Ryerson R, Mahan K, Frierdich G, and Samson L (1987) L-homocysteic acid: an endogenous excitotoxic ligand of the NMDA receptor. *Brain Res Bull* **19:**597-602.

Parisi E, Almadén Y, Ibarz M, Panizo S, Cardús A, Rodriguez M, Fernandez E, and Valdivielso JM (2009) *N*-methyl-D-aspartate receptors are expressed in rat parathyroid gland and regulate PTH secretion. *Am J Physiol Renal Physiol* **296:**F1291-1296.

Patton AJ, Genever PG, Birch MA, Suva LJ, and Skerry TM (1998) Expression of an *N*-methyl-D-aspartate-type receptor by human and rat osteoblasts and osteoclasts suggests a novel glutamate signaling pathway in bone. *Bone* **22:**645-649.

Pavenstädt H, Kriz W, and Kretzler M (2003) Cell biology of the glomerular podocyte. *Physiol Rev* **83:**253-307.

Potter K, Hankey GJ, Green DJ, Eikelboom JW, and Arnolda LF (2008) Homocysteine or renal impairment: which is the real cardiovascular risk factor? *Arterioscler Thromb Vasc Biol* **28:**1158-1164.

Puliti A, Rossi PI, Caridi G, Corbelli A, Ikehata M, Armelloni S, Li M, Zennaro C, Conti V, Vaccari CM, Cassanello M, Calevo MG, Emionite L, Ravazzolo R, and Rastaldi MP (2011) Albuminuria and glomerular damage in mice lacking the metabotropic glutamate receptor 1. *Am J Pathol* **178:**1257-1269.

Rastaldi MP, Armelloni S, Berra S, Calvaresi N, Corbelli A, Giardino LA, Li M, Wang GQ, Fornasieri A, Villa A, Heikkila E, Soliymani R, Boucherot A, Cohen CD, Kretzler M, Nitsche A, Ripamonti M, Malgaroli A, Pesaresi M, Forloni GL, Schlöndorff D, Holthofer H, and D'Amico G (2006) Glomerular podocytes contain neuron-like functional synaptic vesicles. *FASEB J* **20:**976-978.

Reiser J, Polu KR, Möller CC, Kenlan P, Altintas MM, Wei C, Faul C, Herbert S, Villegas I, Avila-Casado C, McGee M, Sugimoto H, Brown D, Kalluri R, Mundel P, Smith PL, Clapham DE, and Pollak MR (2005) TRPC6 is a glomerular slit diaphragm-associated channel required for normal renal function. *Nat Genet* **37:**739-744.

Roselli S, Gribouval O, Boute N, Sich M, Benessy F, Attié T, Gubler MC, and Antignac C (2002) Podocin localizes in the kidney to the slit diaphragm area. *Am J Pathol* **160:**131-139.

Schlöndorff J, Del Camino D, Carrasquillo R, Lacey V, and Pollak MR (2009) TRPC6 mutations associated with focal segmental glomerulosclerosis cause constitutive activation of NFAT-dependent transcription. *Am J Physiol Cell Physiol* **296:**C558-569.

Scott JE, Ruff VA, and Leach KL (1997) Dynamic equilibrium between calcineurin and kinase activities regulates the phosphorylation state and localization of the nuclear factor of activated T-cells. *Biochem J* **324:**597-603.

Sen U, Munjal C, Qipshidze N, Abe O, Gargoum R, and Tyagi SC (2010) Hydrogen sulfide regulates homocysteine-mediated glomerulosclerosis. *Am J Nephrol* **31:**442-455.

Shirato I (2002) Podocyte process effacement in vivo. *Microsc Res Tech* **57:**241-246.

Tian D, Jacobo SM, Billing D, Rozkalne A, Gage SD, Anagnostou T, Pavenstädt H, Hsu HH, Schlondorff J, Ramos A, and Greka A (2010) Antagonistic regulation of actin dynamics and cell motility by TRPC5 and TRPC6 channels. *Sci Signal* **3:**ra77

Tyagi N, Vacek JC, Givvimani S, Sen U, and Tyagi SC (2010) Cardiac specific deletion of *N*-methyl-D-aspartate receptor 1 ameliorates mtMMP-9 mediated autophagy/mitophagy in hyperhomocysteinemia. J *Recept Signal Transduct Res* **31:**78-87.

Wang L, Chang JH, Paik SY, Tang Y, Eisner W, and Spurney RF (2011) Calcineurin (CN) activation promotes apoptosis of glomerular podocytes both in vitro and in vivo. *Mol Endocrinol* **25:**1376-1386.

Wang Y, Jarad G, Tripathi P, Pan M, Cunningham J, Martin DR, Liapis H, Miner JH, and Chen F (2010) Activation of NFAT signaling in podocytes causes glomerulosclerosis. *J Am Soc Nephrol* **21:**1657-1666.

Wang Z, Wei X, Zhang Y, Ma X, Li B, Zhang S, Du P, Zhang X, and Yi F (2009) NADPH oxidase-derived ROS contributes to upregulation of TRPC6 expression in puromycin aminonucleoside-induced podocyte injury. *Cell Physiol Biochem* **24:**619-626.

Winn MP, Conlon PJ, Lynn KL, Farrington MK, Creazzo T, Hawkins AF, Daskalakis N, Kwan SY, Ebersviller S, Burchette JL, Pericak-Vance MA, Howell DN, Vance JM, and Rosenberg PB (2005) A mutation in the TRPC6 cation channel causes familial focal segmental glomerulosclerosis. *Science* **308:**1801-1804. .

Yi F, dos Santos EA, Xia M, Chen QZ, Li PL,and Li N (2007) Podocyte injury and glomerulosclerosis in hyperhomocysteinemic rats. *Am J Nephrol* **27:**262-268.

Zhang C, Yi F, Xia M, Boini KM, Zhu Q, Laperle LA, Abais JM, Brimson CA, and Li PL(2010a) NMDA receptor-mediated activation of NADPH oxidase and glomerulosclerosis in hyperhomocysteinemic rats. *Antioxid Redox Signal* **13:**975-986.

Zhang C, Hu JJ, Xia M, Boini KM, Brimson C, and Li PL (2010b) Redox signaling via lipid raft clustering in homocysteine-induced injury of podocytes. *Biochim Biophys Acta* **1803:**482-491.

Zhang C, Xia M, Boini KM, Li CX, Abais JM, Li XX, Laperle LA, and Li PL (2011) Epithelial-to-mesenchymal transition in podocytes mediated by activation of NADPH oxidase in hyperhomocysteinemia. *Pflugers Arch* **462:**455-467.

Zhu ZT, Munhall A, Shen KZ, and Johnson SW (2005) NMDA enhances a depolarization-activated inward current in subthalamic neurons. *Neuropharmacology* **49:**317-327.

Molecular Pharmacology Fast Forward. Published on July 24, 2012 as DOI: 10.1124/mol.112.079376
This article has not been copyedited and formatted. The final version may differ from this version.

Footnotes.

This work was supported by National Institute of Diabetes and Digestive and Kidney Diseases [RO1-DK-8259]; and an American Society for Nephrology James M. Scherbenske Award.

Author for correspondence. Dr. Stuart Dryer, Department of Biology and Biochemistry, University of Houston, 4800 Calhoun, Houston, TX, 77204-5001 USA.

Molecular Pharmacology Fast Forward. Published on July 24, 2012 as DOI: 10.1124/mol.112.079376
This article has not been copyedited and formatted. The final version may differ from this version.

Figure legends

Figure 1. NMDA treatment increases generation of ROS and mobilization of $p47^{(phox)}$ in a podocyte cell line.

(A) Increase in H_2O_2 generation in podocytes treated with 100 μM NMDA for 24-72 hr is quenched by concurrent exposure to 100 μM MnTBAP, a scavenger of ROS. NMDA treatment for 6 hr was not sufficient to produce an increase in bulk cytosolic H_2O_2 large enough to be detected by this fluorometric assay. In this and subsequent figures, bar graphs denote mean ± s.e.m. (B) Representative cell-surface biotinylation assay showing increase in steady-state surface expression of $p47^{(phox)}$ after 24-hr exposure to 100 μM NMDA. This effect was completely blocked by concurrent exposure to 10 μM MK-801. (C) Densitometric analysis of three repetitions of the experiment illustrated in B.

Figure 2. NMDA treatment evokes an increase in steady-state surface expression of podocyte TRPC6 channels.

(A) Representative cell surface biotinylation assays showing surface expression of TRPC6 after 24 hr of NMDA exposure at the concentrations indicated. Note robust effects of NMDA at 50 and 100 μM. (B) The effect of 24-hr exposure to 100 μM NMDA is completely inhibited by concurrent exposure to 10 μM MK-801. (C) Densitometric analysis of three repetitions of the experiment shown in B. (D) The effect of 100 μM NMDA is also inhibited by concurrent exposure to 100 μM of the ROS scavenger MnTBAP. (E) Densitometric analysis of three repetitions of the experiment shown in D.

Molecular Pharmacology Fast Forward. Published on July 24, 2012 as DOI: 10.1124/mol.112.079376
This article has not been copyedited and formatted. The final version may differ from this version.

Figure 3. NMDA treatment increases TRPC6-like cationic currents in podocytes. All cells were treated with 100 μM OAG for 15 min before recordings were made. (A) Examples of whole-cell currents evoked by ramp voltage commands (-80 mV to +80 mV in 2.5 seconds) made from a holding potential of -40 mV. Traces on left show currents before and after bath superfusion of 50 μM La^{3+}, and traces on right are digital subtractions (control — La^{3+}). Examples shown are from control cells and from cells treated for previous 24 hr with 100 μM NMDA in presence and absence of 10 μM MK-801 or 100 μM MnTBAP, as indicated. NMDA was not present at the time recordings were made. Note increase in La^{3+}-sensitive currents in NMDA-treated cells, and inhibition of this effect by MK-801 and MnTBAP. (B) Summary of results of recordings with n = 10 cells in each group. Ordinate represents La^{3+}-sensitive current measured at +80 mV. Asterisk indicated $P < 0.05$ as determined by one-way ANOVA followed by Tukey's post hoc test. (C) As in panel A except that traces show currents evoked before and after application of 50 μM SKF-96365.

Figure 4. NMDA increases nuclear localization of NFAT in podocytes. (A) NMDA treatment for 24 hr increases the amount of NFAT detected by immunoblot in a nuclear extract of podocytes. Histone expression was used to monitor loading. There was no change in NFAT expression in the cytosolic fraction in which actin expression was used to monitor loading. The effects of NMDA were blocked by either 10 μM MK-801 or 10 μM SKF-96365, an inhibitor of TRPC6 channels. (B) Densitometric analysis of three repetitions of the experiment shown in A. (C) Confocal

Molecular Pharmacology Fast Forward. Published on July 24, 2012 as DOI: 10.1124/mol.112.079376
This article has not been copyedited and formatted. The final version may differ from this version.

images of popdocytes showing expression of NFAT (red) and DAPI-stained nuclei (blue). Note concentration of NFAT in nuclei after 24 hr NMDA treatment, and inhibition of this effect by MK-801 and SKF-96365.

Figure 5. NMDA stimulation of nuclear NFAT expression in podocytes is blocked by cyclosporine.

Using the methods described in the previous figure, we observed that NMDA effects were blocked by concurrent exposure to 10 μM cyclosporine (CsA), as assessed by immunoblot (A) and confocal (B) detection of nuclear NFAT.

Figure 6. Effects of NMDA on activation of small GTPases in podocytes.

(A) Representative glutathione-*S*-transferase pull-down assay (left) and densitometric analysis of three repetitions of this assay (right) showing that 24-hr exposure to 100 μM NMDA evokes activation of RhoA but does not affect total RhoA. (B) NMDA treatment does not change levels of activated or total Rac1.

Figure 7. NMDA treatment reduces total and surface expression of podocyte markers. Cells were treated with 100 μM NMDA for 24 hr and total and surface expression of nephrin and podocin were analyses using cell-surface biotinyation assays. Actin was used as a separate loading control. NMDA treatment caused a reduction in total expression of both nephin and podocin relative to actin. This treatment caused even larger reductions in the amount of these proteins that could be detected at the cell surface. (A) A representative example of this experiment. (B) Densitometric analysis

of three repetitions of this experiment. All signals in the ordinate are normalized to total actin.

Figure 8. More prolonged NMDA treatment causes loss of viable podocytes. (A) A 24-hr treatment with 100 μM NMDA did not affect podocyte viability as assessed by dye-exclusion procedures, but 72-hr treatments reduced cell viability. (B) A similar pattern was observed by monitoring release of lactate dehydrogenase into the medium, and the effect of 72-hr treatment with NMDA was blocked by concurrent exposure to MK-801. (C) Treatment with NMDA for 72 hr evoked DNA fragmentation as assessed by TUNEL staining of nuclei (green fluorescence). This was not seen in control cells or in cells exposed to NMDA for 24 hr. In these images, nuclei are counterstained using DAPI (blue fluorescence). (D) A 72-hr exposure to 100 μM NMDA increased expression of apoptotic markers caspase 3, caspase 6 and Bax, and caused a modest decrease in Bcl-Xl

Figure 9. An endogenous agonist of NMDA receptors also mobilizes podocyte TRPC6 channels and evokes nuclear fragmentation. (A) Representative cell surface biotinylation assay showing increase in steady-state surface expression of podocyte TRPC6 channels after 24 hr exposure to 50 μM L-HCA. (B) Densitometric analysis of three repetitions of the experiment shown in A. (C) TUNEL assays of nuclear fragmentation in control podocytes and in podocytes treated with 50 μM L-HCA for 72 hr.

Figure 1

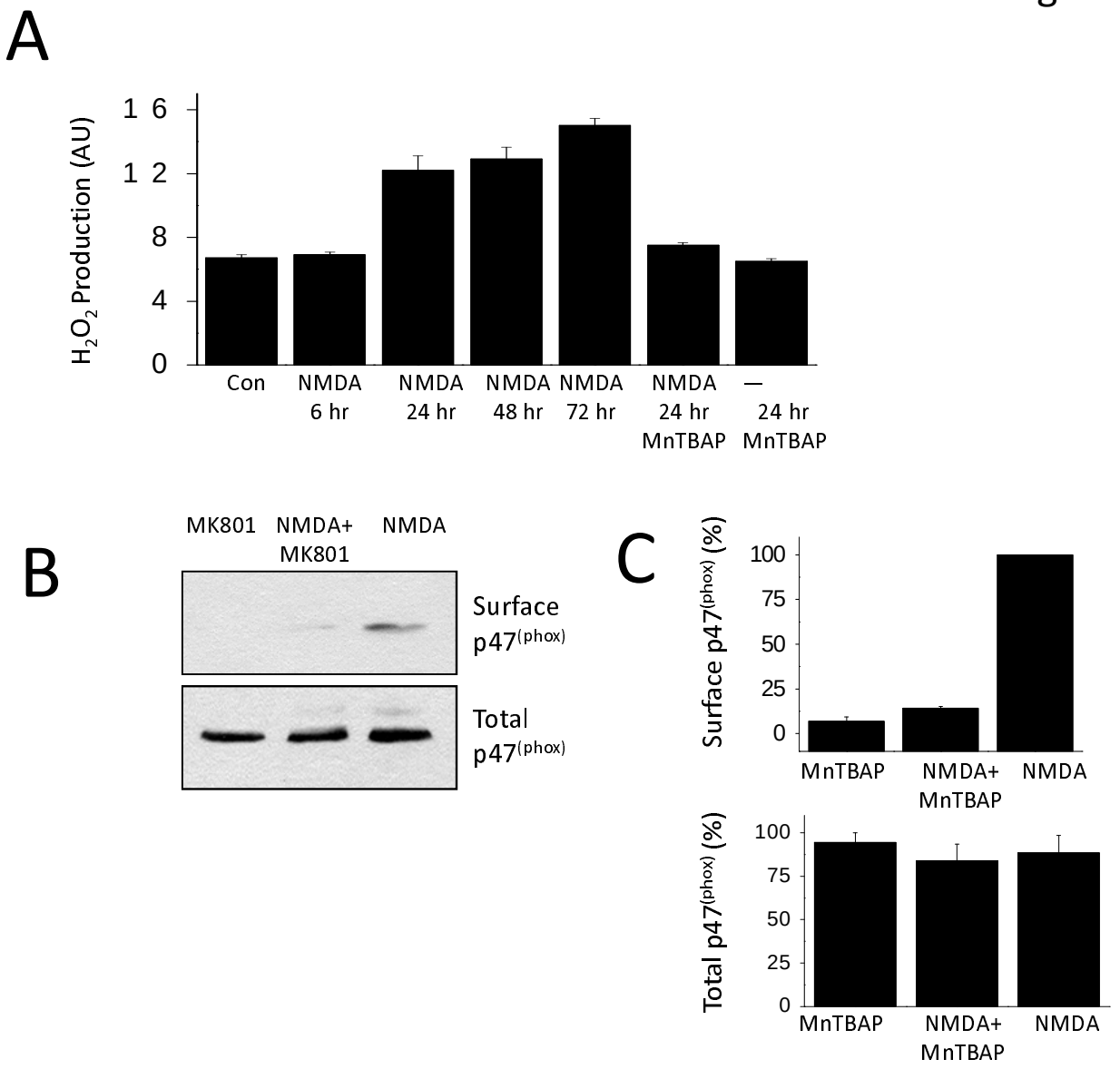

Figure 2

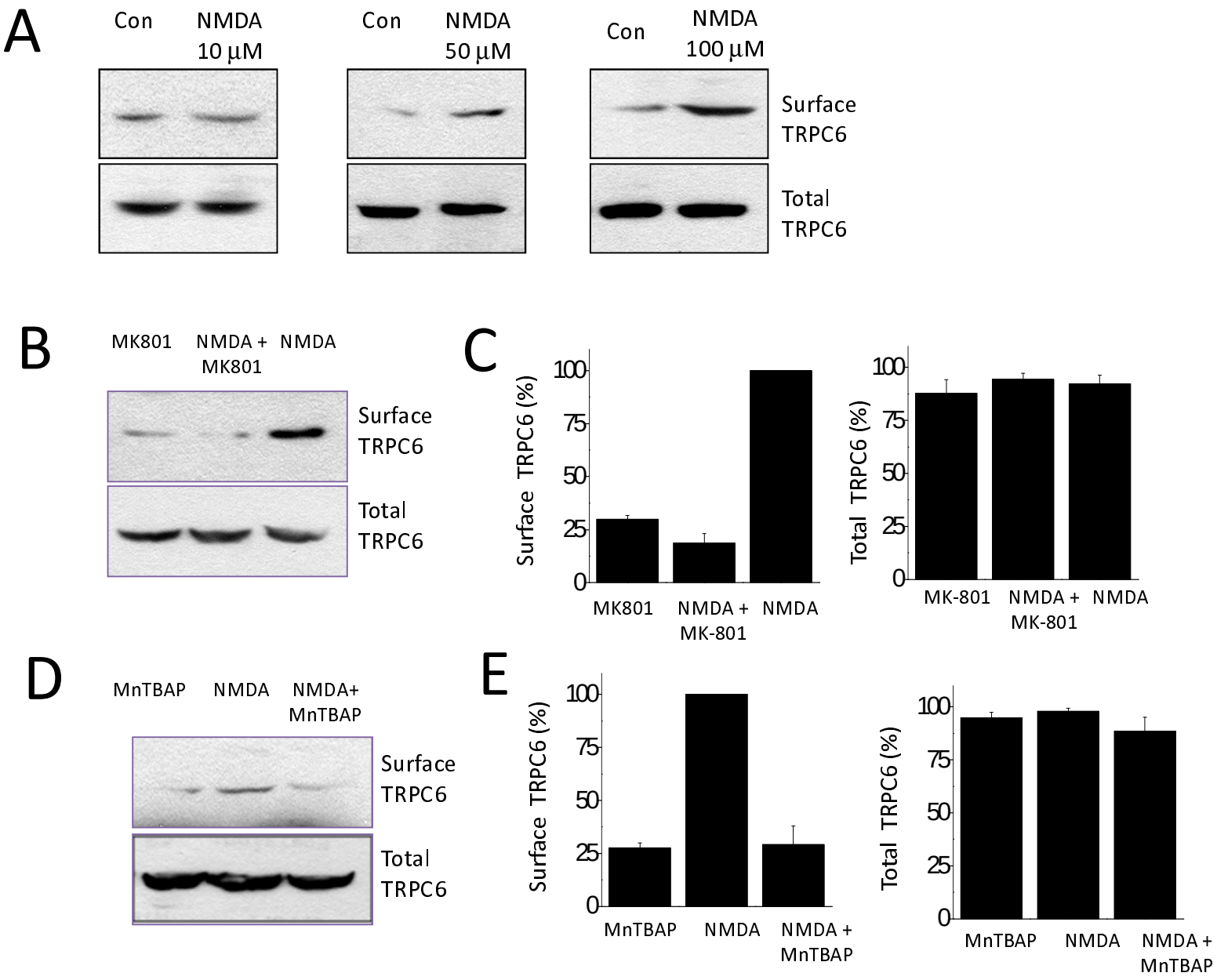

Figure 3

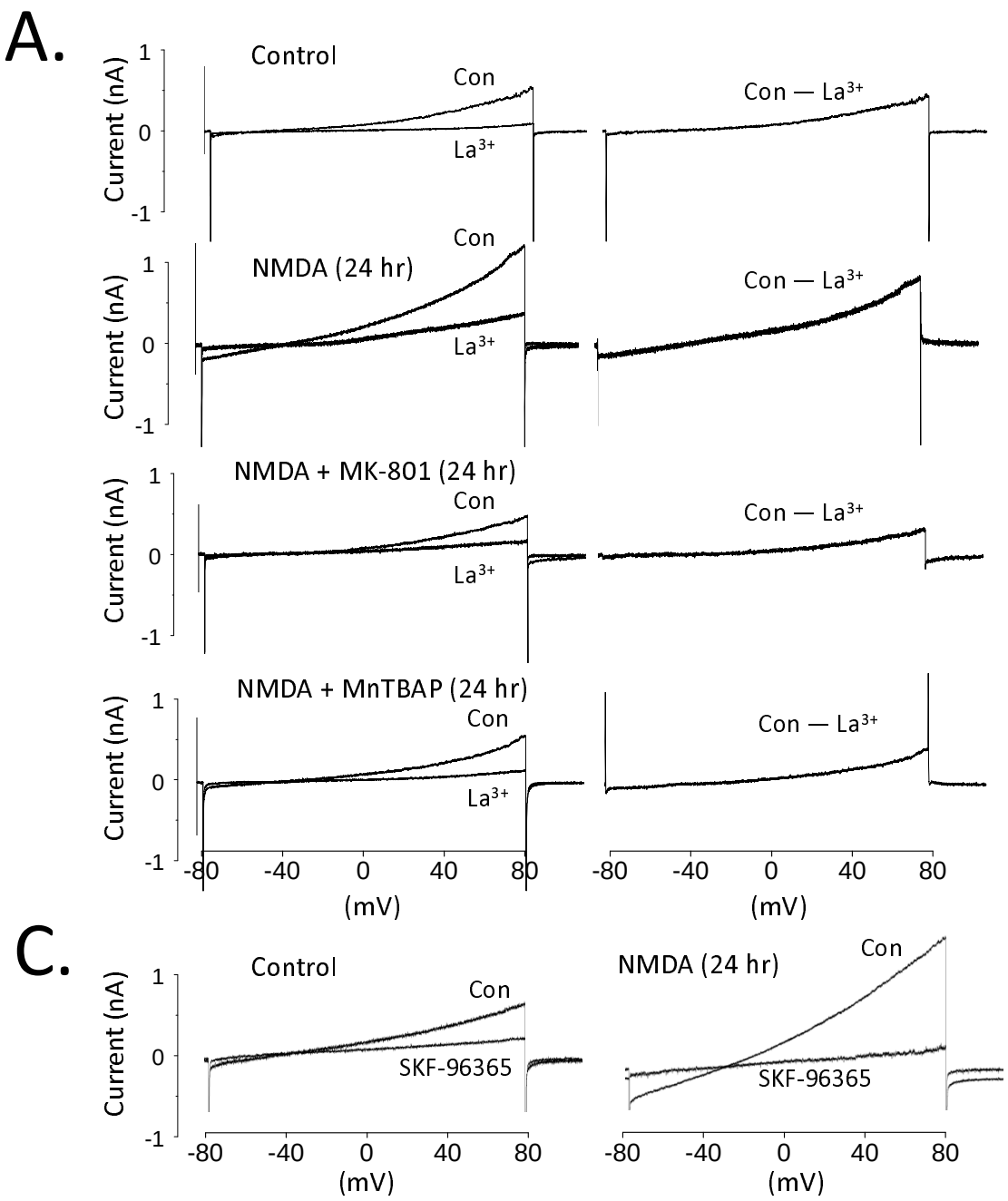

Figure 4

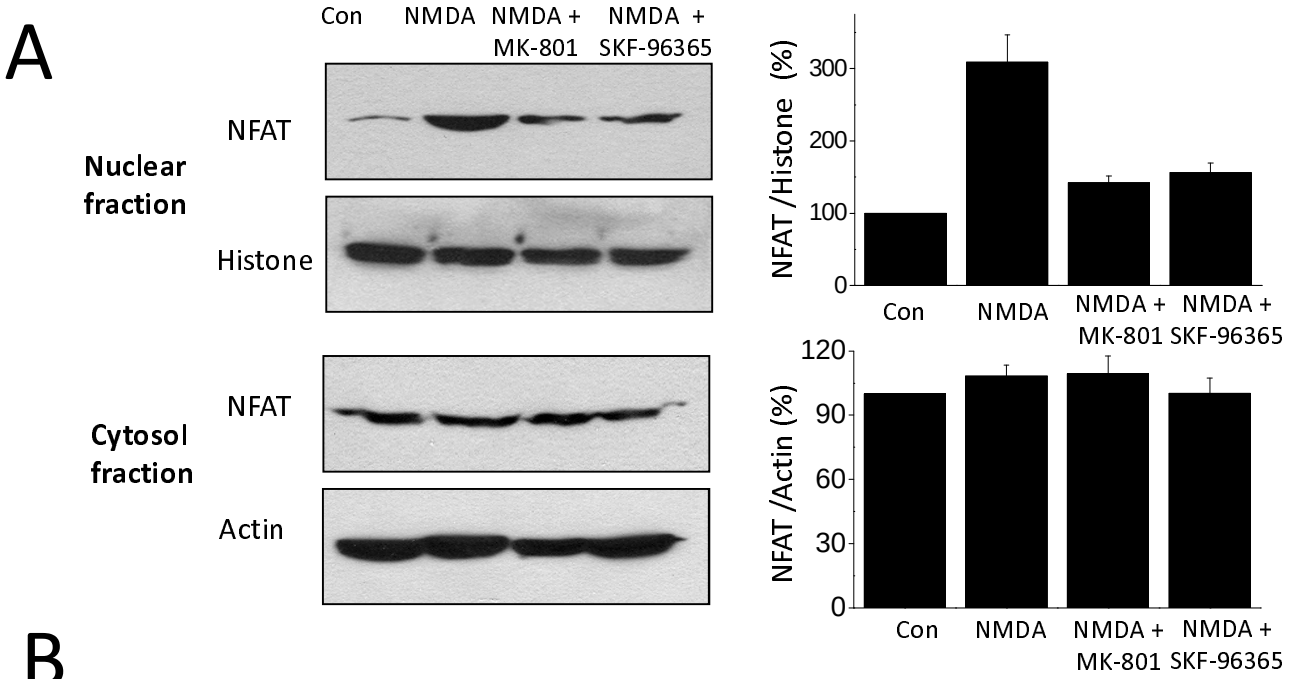

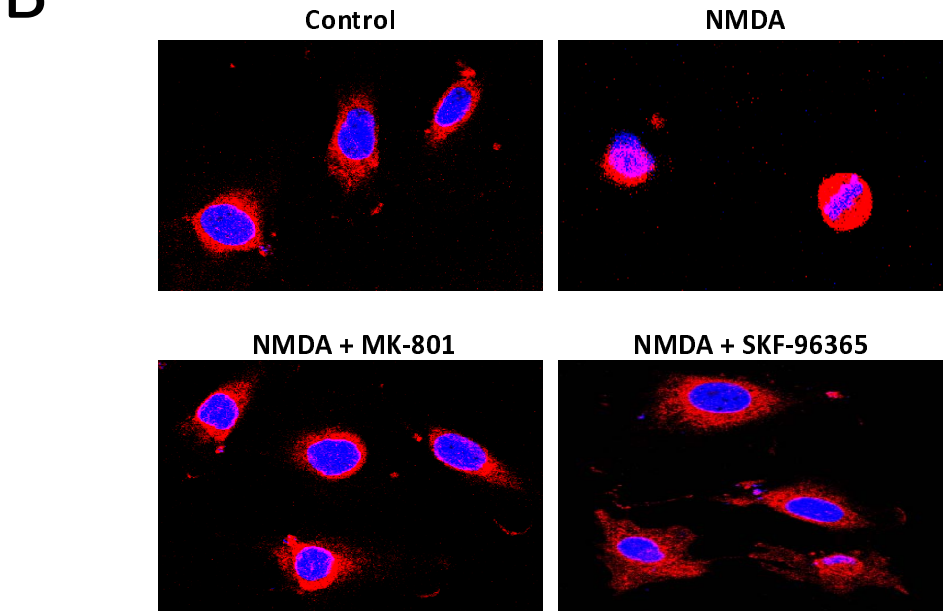

Figure 5

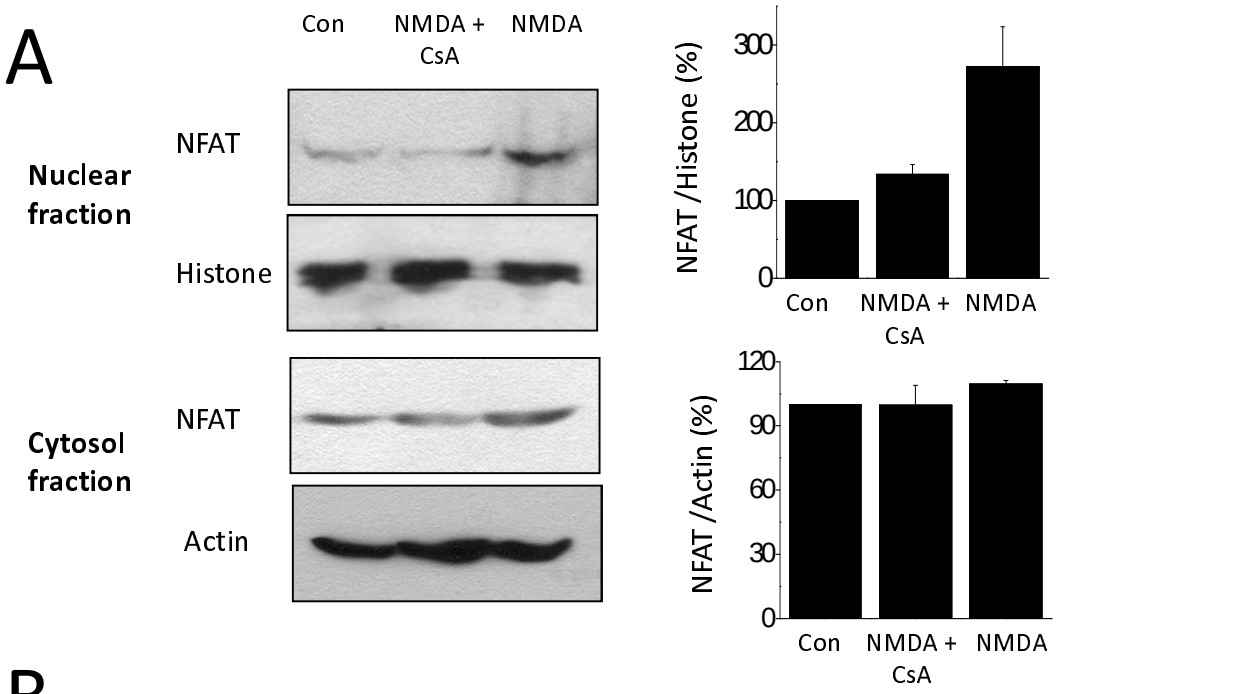

Figure 6

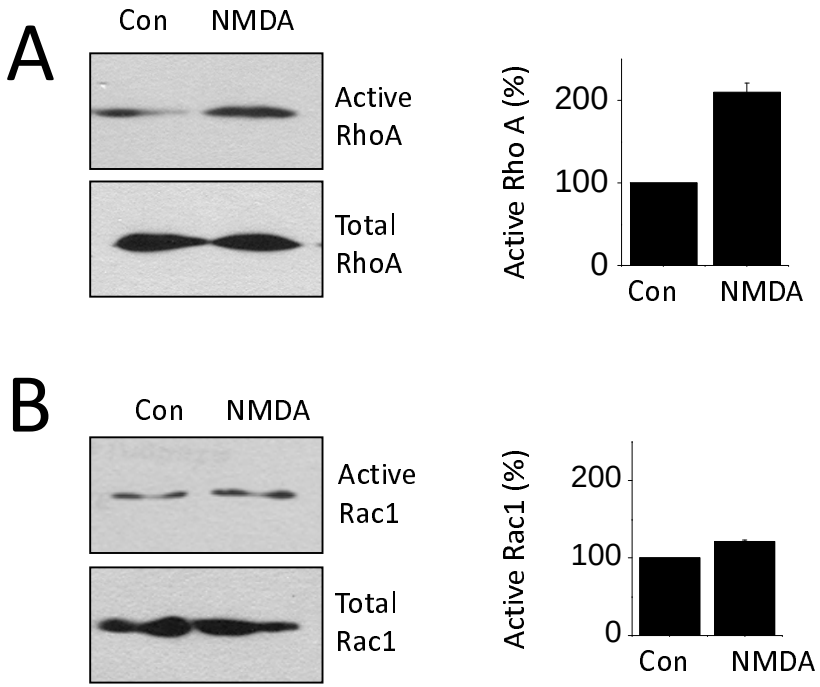

Figure 7

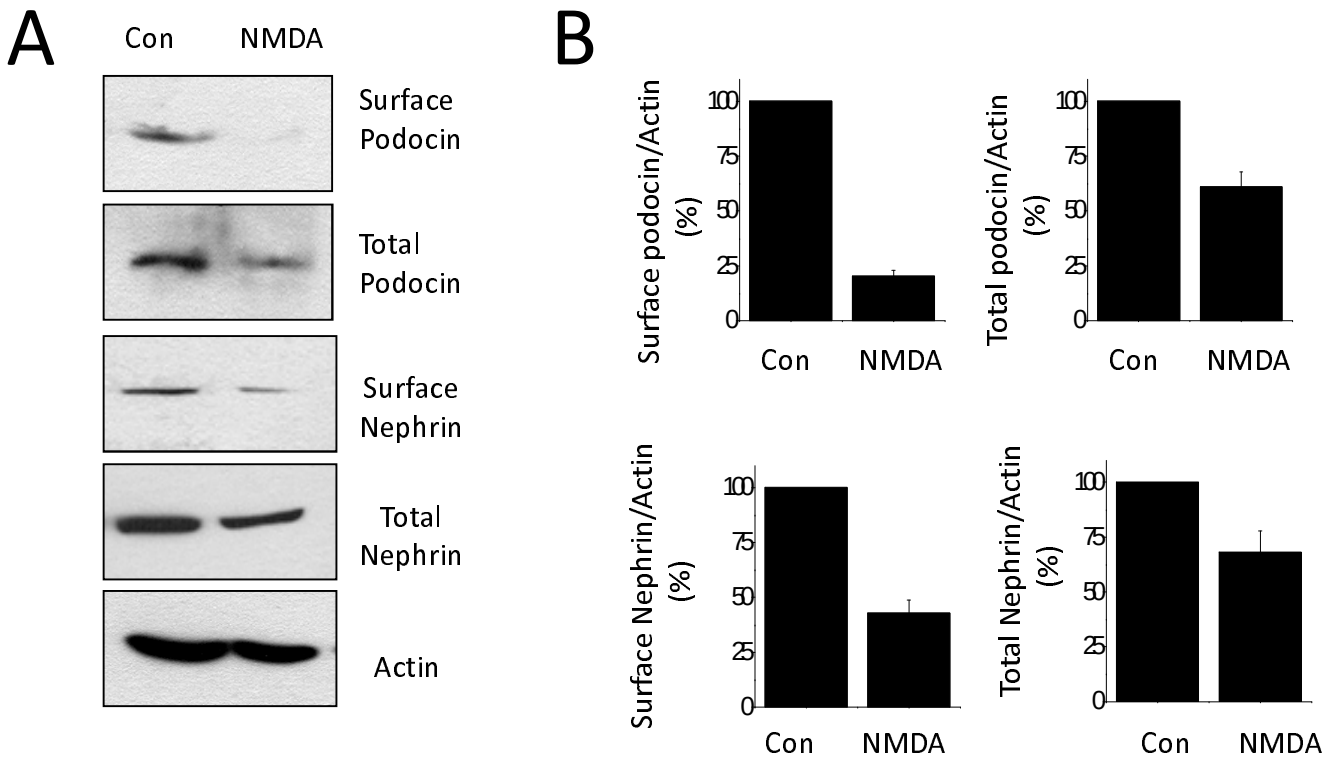

Figure 8

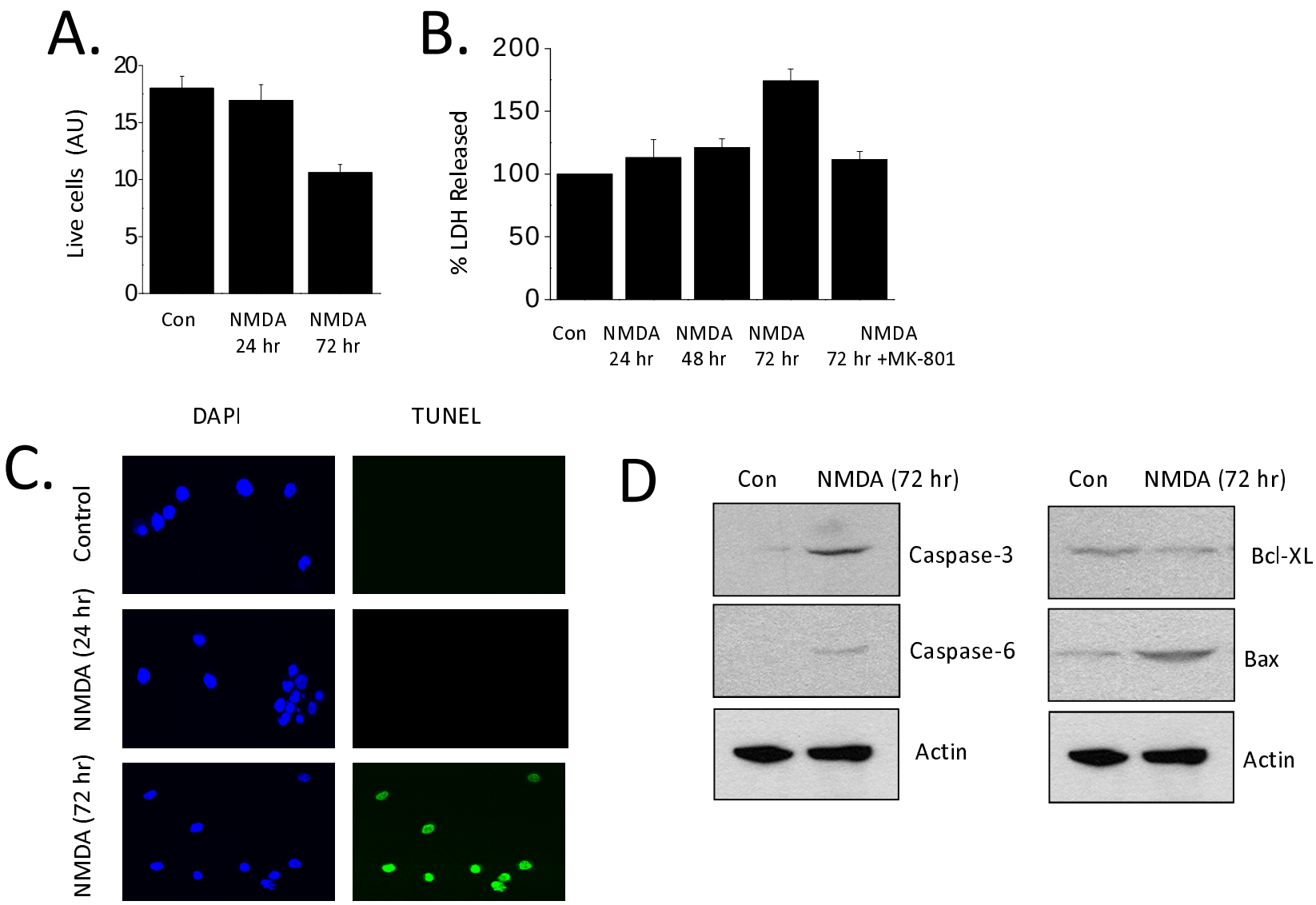

Figure 9